 doi:10.20944/preprints202203.0382.v1

Type of the Paper (Article)

The Characteristic of CFRP Laminates Related to Water Absorption Subjected to Tensile, Bending, and Compression

Sudarisman[1], Alfian Hidayat[2], Haniel[1], Muhammad Tiopan[1], Rela Adi Himarosa[1], and Muhammad Akhsin Muflikhun[3,4,*]

[1] Mechanical Engineering Department, Universitas Muhammadiyah Yogyakarta, Indonesia; sudarisman@umy.ac.id
[2] Asahikawa National College of Technology; Japan; alfianmfh@gmail.com
[3] Mechanical and Industrial Engineering Department Gadjah Mada University, Indonesia; akhsin.muflikhun@mail.ugm.ac.id
[3] Center for Advanced Manufacturing and Structural Engineering (CAMSE), Gadjah Mada University, Indonesia.

* Correspondence: akhsin.muflikhun@ugm.ac.id; Tel.: +6281327181945

Abstract: This research aims to investigate the carbon fiber reinforced polymer (CFRP) when subjected to tensile, bending, and compression. Half of the specimens are also subjected to water to find out how water influences. The CFRP is created using a combination of carbon fiber layers and epoxy resin Bisphenol A Epichlorohydrin with hardener and is formed using the vacuum infusion method. From the water absorption test, it was found that the average weight gain of the specimens was 2.9% and the lowest value was at 0.6%, it was concluded that the increase in wet specimen weight was not too significant and water absorption tended to be slow. Mechanical testing obtained the highest average tensile stress, bending stress, compressive stress, and modulus of elasticity of 195 MPa, 295 MPa, 96 MPa, and 8914 MPa were from dry specimens while the lowest average values were 146 MPa, 286 MPa, 81 MPa, and 6160 MPa from wet specimens. The results of micro-photo observations on the tensile test fracture show that the specimen has a XGM fracture character with delamination and splitting fractures happening in multiple areas. In the bending test, the specimens experienced buckling fracture due to the fiber breaking and the inability of the matrix to withstand the additional stress. Shear fracture happened during the compressive test. In conclusion, water absorption has a bad impact towards the composite strength.

Keywords: CFRP, vacuum infusion, water absorption, tensile test, bending test, compressive test

1. Introduction

The use of composite materials in everyday life varies greatly, from the manufacture of household appliances, engine components, ships, and car bodies made of polymer composite materials. The advantages of the composites materials compared with metal-based materials can be found in their superior properties such as; great corrosion resistance, outstanding strength to weight ratio, and excellent results in static and fatigue tests [1–4]. Other properties of composites that also has a smaller density and a greater hardness value [5–7]. If more parts of the vehicle are made of composites, the overall weight of the vehicle will be lighter which results in a better fuel efficiency [8]. The advantages of this composite material are suitable for use in the automotive, shipping and aircraft industries [9–11].

To produce high-quality composite vehicle components, it is necessary to take a closer look at the characterization of the materials used in the manufacture of composites. Carbon fiber has advantages over other fibers in the manufacture of composites. Carbon fiber generally has a high tensile strength value, low density, low thermal and electrical

 doi:10.20944/preprints202203.0382.v1

conductivity and good creep resistance [12–14]. Carbon fiber can maintain its structure and properties under extreme fluid, pressure, and temperature conditions. The application of carbon fiber to vehicle components can even reduce vehicle weight and will result in lower fuel consumption. The addition of carbon fiber is also able to increase the attenuation of sound and vibration in the cabin to provide comfort and safety to the passengers. This is due to carbon fiber low density, high tensile modulus and its resistant to high temperatures [15]. However, carbon fiber has a low compressive strength [16,17]. To overcome this conditions, carbon fiber is combined with polymer to create carbon fiber reinforced polymers (CFRP), a strong polymer composite, was used. The matrix polymer also used as the glue to keep the carbon fiber and glass fiber stick together [18,19]. The polymer used in CFRP is generally an epoxy resin, a thermoset polymer, which is formed through a condensation polymerization process, a plastic material that cannot be re-softened or reshaped to a state before drying. The manufacturing process can be carried out at room temperature by considering the chemical substances used as controllers of cross-link polymerization in order to obtain optimum results. Epoxy belongs to a group of polymers that are used as coatings, adhesives, and as a matrix in composite materials in several structural parts, these resins are also used as a mixture of packaging materials, molding materials, and adhesives [20–22].

Epoxy resin has the properties of an amorphous structure, cannot be melted, cannot be recycled, and the atoms are strongly bonded. The advantages of this epoxy resin are its resistance to heat and moisture, good mechanical properties, resistance to chemicals, insulating properties, good adhesive properties against various materials, and this resin is easy to modify and manufacture. However, epoxy also has the disadvantage of being sensitive to water and brittle. The use of epoxy as a matrix material is limited by its low toughness and brittleness [17,23,24]. Several studies on the use of composites as vehicle components have been carried out, such as that of Sunardi, et al. [25] by examining the tensile strength of pandanus palm tree leaf fibers for motor vehicle body applications. The results showed that the greatest tensile strength was obtained in the composite with the vertical fiber direction, at 20.741 N/mm^2. While the smallest tensile strength is obtained in the composite with horizontal fiber direction, at 17.955 N/mm^2. The results of the microphotographs showed that the composites with ductile fractures were composites with vertical and random fiber directions, while composites with horizontal and cross fiber directions had brittle fractures. Masdani, et al. [25] studied the development of agarwood fiber-reinforced composites as a substitute for fiberglass in the manufacture of car dashboards using the hand lay-up method. The maximum value of tensile strength is 34.574 MPa in the fiber volume fraction of 45%. Using SEM (Scanning Electron Microscope), in specimens with volume ratio of 40% and 50% at the fracture section, some of the fibers were pulled out from their bonds. This causes imperfect bonds between the fibers to the matrix because the presence of lignin between the fibers. The fibers are released because the bonds between the fibers and the matrix are more dominant on one side. Hanifi, et al. [25] have conducted research on the analysis of the mechanical and physical properties of oil palm midrib fiber composites as car bumpers. The results showed that the maximum tensile strength was obtained at the volume fraction of 40% fiber and 60% matrix with a value of 21.106 MPa and elastic modulus of 2323.9 MPa. It was concluded that the addition of fiber composition and arranged in a regular manner could increase the tensile strength of the composite and the modulus of elasticity. Other researchers investigated the effect of fiber length and volume fraction on the impact and bending strength of composite materials using the compressing molding method. From the bending test on two different types of fiber, it was found that the synthetic fiber was stronger than natural fiber with the highest value of the polyester-fiber glass composite bending test obtained [26,27]. Previous study compared the characteristics of carbon fiber between the manual layup and vacuum infusion methods with the use of 60% fiber weight fraction [28]. Vacuum infusion is a method of making composite materials through a closed molding process. The working principle of vacuum infusion involves the use of atmospheric pressure as a means of

Preprints (www.preprints.org) | NOT PEER-REVIEWED | Posted: 29 March 2022 doi:10.20944/preprints202203.0382.v1

suppression. Vacuum infusion has an inlet and outlet that is used to flow the resin. It was found that the strength of the carbon fiber composite using the vacuum infusion method is stronger than the manual lay-up method with an average tensile strength of 595.63 MPa with an elastic modulus of 6.976 MPa with an average impact strength of 33.25 J/cm2 and energy absorbed 2,433.65 J. Using the lay-up method, the tensile strength is 581.93 MPa, the modulus of elasticity is 10.241 MPa, and the average impact strength is 29.41 J/cm² and the amount of energy absorbed is 2.212.59 J. This is because the vacuum process produces a more even distribution of the matrix, thereby minimizing the appearance of voids in the composite.

The characterization of the fiber tend to have different perspective to the different people. The increase application of composites in different sector can give opportunity to aerospace and automotive applications. However, this condition also have implication to the other industries. To determine the effect of the CFRP that subjected to water absorption, several studies are used by researchers. The present study investigate the effect of water absorption on the CFRP laminates subjected to different tests which are tensile, bending, and compression. This study can be used to determine the behavior and the physical effect of the CFRP that in the future can be applied in different applications.

2. Materials and Methods

2.1. Materials and Tools

1. Matrix and Hardener

Figure 1. Bisphenol A matrix and hardener.

The matrix used is Bisphenol A Epoxy Resin with the property below.

Table 1. Bisphenol A Epoxy Resin property

Properties	Unit	Value
Viscosity	mPa	13.000 ± 2.000
Epoxy number	%	22.7 ± 0.6
Epoxy equivalent	g/equiv	189 ± 5
Epoxy value	Equiv/100 g	0.53 ± 0.01
Total chlorine content	%	<0.2
Hidrolyzable chlorine content	%	<0.05
Colour according to the gardner scale		<1
Density at 25°C	g/cm³	1.17 ± 0.01
Refractive index at 25°C		1.572 ± 0.003
Volatile content at 3h, 140°C	%	<0.2
Vapour preassure at 80°C	mbar	<0.1
Flashpoint according to DIN 51584	°C	>250

Preprints (www.preprints.org) | NOT PEER-REVIEWED | Posted: 29 March 2022 doi:10.20944/preprints202203.0382.v1

2. Carbon Fiber

Figure 2. Carbon fiber fabric.

Commercial grade 2×2 twill weave carbon fiber fabric with the following specification is used.

Table 2. Carbon Fiber Fabric Property

Items		**200 gr/m²**
Weave		Twill
Width		1500 ± 5mm
Area weight		200 ± 5 gr/m
Thickness		0,28 ± 0,02 mm
Density (ends/100mm)	Warp	50 ± 2
	Wave	50 ± 2
Breaking strength (n/25mm)	Warp	> 1000
	Wave	> 1000

3. Mirror Glaze

Mirror Glaze serves to polish the surface of the composite and facilitate the removal of the composite from the mold.

4. Molding Surface

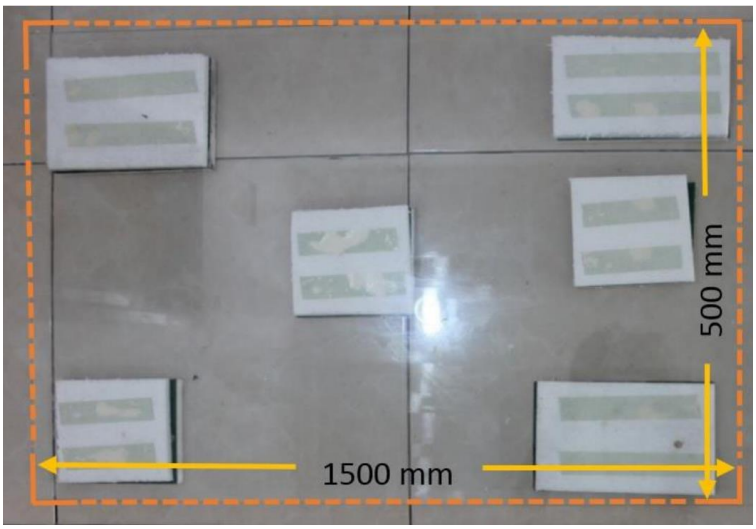

Figure 3. Molding surface.

The mold used in this study uses flat glass with a length of 1500 mm, a width of 500 mm, and a thickness of 5 mm. The bottom surface of the mold is cushioned made of

 doi:10.20944/preprints202203.0382.v1

Styrofoam material for easy movement and is useful for protecting the glass from breaking when placed on a hard surface. This mold is used as a surface for the specimen molding process using vacuum infusion so that the specimen molding results are flat and prevent wavy molding results.

5. Vacuum Compressor

   A vacuum compressor is used to flow the resin into the mold so that it wets the fibers.

6. Resin Reservoir

   The reservoir tube functions as a place to accommodate the remaining sucked matrix and prevent the sucked matrix from reaching the vacuum compressor. The reservoir tube is also equipped with a pressure gauge indicator that indicates the suction pressure used during the molding process.

7. Bagging Film

   This component functions as a cover on all sides of the mold and as a vacuum chamber, is placed on the top surface and attached to the surface of the mold by using a sealant tape.

8. Flow Media

   This component serves to facilitate the flow of the matrix to the entire surface of the fiber and avoid sticking between the fiber and the bagging film.

9. Peel Ply

   Peel ply is used as a separator between the flow media and the fiber to avoid sticking between these components. The peel ply will be removed from the composite material when molding is finished.

10. Spiral Hose and T-Connectors

    Spiral hoses are used so that the flowing matrix can distribute the flow evenly and avoid the matrix from flowing on one side. T-connector is used as a connection to the spiral hose. Two T-connectors are used as resin inlet and outlet.

2.2. Methods

2.2.1. Water Absorption Test

The resistance of composite materials in an aqueous environment is largely determined by the ability of the composite to absorb water from the environment. The more water absorbed, the less strong the fiber and matrix interface bonds, and vice versa (Tododjahi et al, 2014). A simple method for assessing water absorption is by measuring changes in sample weight before and after immersion

water.

The test in this study was a water absorption test which was carried out for 12 hours and then tested for tensile strength. Water absorption is one of the causes of the change in the mechanical strength of the composite because the fiber properties that absorb water that cannot be removed from the fiber-reinforced composite. This absorption causes the bonds between the fibers and the matrix to weaken (Sasdiwijantara et al, 2019). The weight gain of the composite was recorded and then the percentage was calculated using the equation and the thickness increase using the following equation:

$$\text{water absorption} = (\text{final mass} - \text{initial mass}) / (\text{initial mass}) \times 100\% \quad (1)$$

2.2.2. Tensile Test

In the vacuum infusion process, the fiber and flow media are placed on top of the mold and then closed using a vacuum bag film, then the air in the mold and composite is expelled into the atmosphere with the help of a vacuum pump. This process will produce a composite that has a high matrix to reinforcement ratio, uniform mechanical properties, fewer voids, and a uniform matrix thickness. This study used ASTM D638-14 and the details of the specimen sizes are as follows:

Preprints (www.preprints.org) | NOT PEER-REVIEWED | Posted: 29 March 2022 doi:10.20944/preprints202203.0382.v1

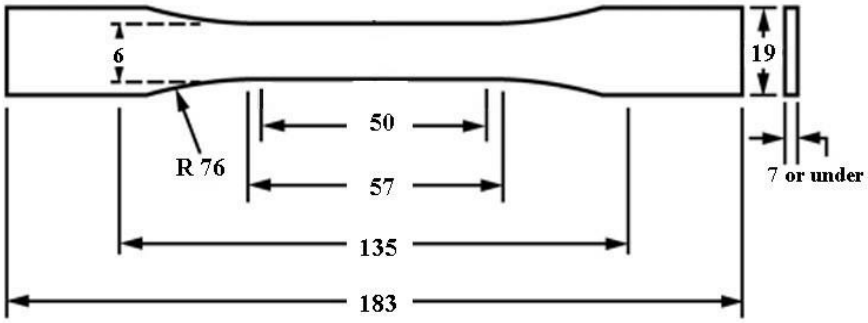

Figure 4. Specimen cross section [29].

Table 3. Specimen dimensions.

Symbol	Information	Type II (7 cm or under)
W	Width of narrow section	6 mm
L	Length of narrow section	57 mm
WO	Width overall	19 mm
LO	Length overall	183 mm
D	Distance between grips	135 mm
R	Radius of fillet	76 mm
G	Gage length	50 mm

During tensile loading, failure that can happen can be classified into several characteristics which are described in ASTM D3039 standard depicted below.

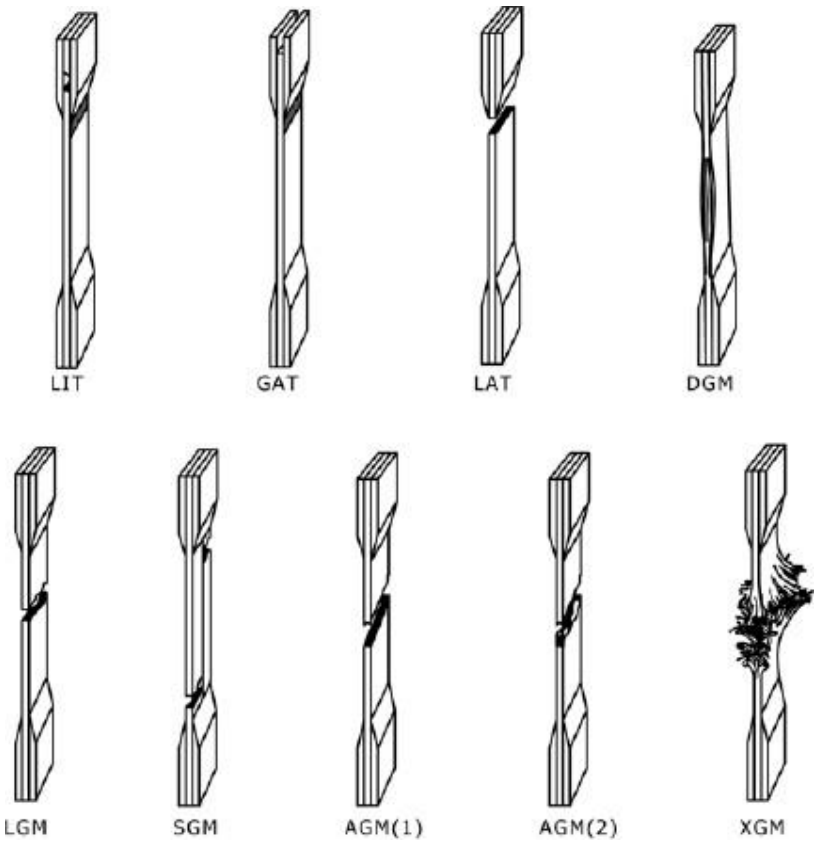

Figure 5. Failure characteristics [30].

Preprints (www.preprints.org) | NOT PEER-REVIEWED | Posted: 29 March 2022 doi:10.20944/preprints202203.0382.v1

Table 4. Failure characteristics code.

First Character		Second Character		Third Character	
Failure Type	Code	Failure Type	Code	Failure Type	Code
Angled	A	Inside grip/tab	I	Bottom	B
edge Delamination	D	At grip/tab	A	Top	T
Grip/tab	G	<1W from Grip/tab	W	Left	L
Lateral	L	Gage	G	Right	R
Multi Mode	M	Multi Areas	M	Middle	M
Long Splitting	S	Various	V	Various	V
Explosive	X	Unknown	U	Unknown	U
Other	O				

The reading of the fault characteristic code in the image based on the letters arranged shows the meaning of the occurring fault character. For example, a characteristic with DGM code has a D-edge delamination type failure, a G-gage failure area (at the gage length), and middle fault location (M-middle). Classification of fracture character above aims to determine the type of failure that is allowed or specimens that fall into the permitted category. The allowed fault categories are LGM, SGM, AGM (1), AGM (2), XGM.

2.2.3. Bending Test

The load bending test aims to determine the bending stress (σ), angular deflection formed by bending (δ), and elasticity (E). The bending test is done according to the ASTM D790 standard three point bending test, with the dimension of specimen specified below.

Table 5. Specimen dimensions.

Symbol	Information	Value
P	Length	50.8 mm
L	Width	12.7 mm
T	Thickness	1.6 mm

2.2.4. Compression Test

The test standard used is the form of a compression the specimen based on the ASTM D695 standard. The thickness of the specimen is 3.2 mm. The shape and size of the test specimen is specified below.

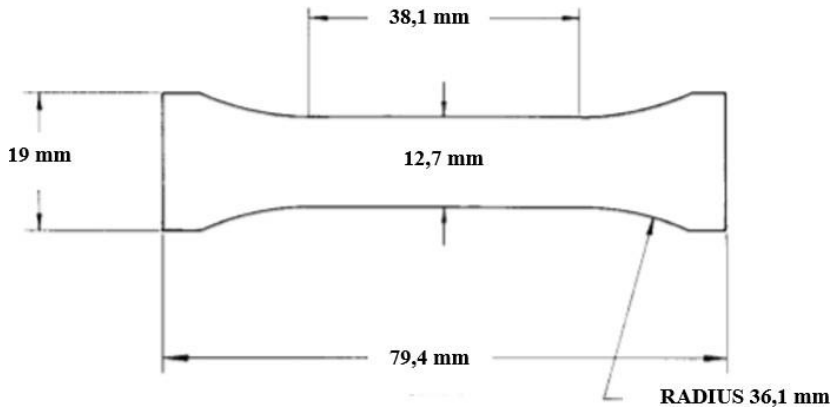

Figure 6. Specimen dimensions [31].

Preprints (www.preprints.org) | NOT PEER-REVIEWED | Posted: 29 March 2022 doi:10.20944/preprints202203.0382.v1

2.3 Manufacturing Processes

The figure below depicts the schematic diagram of the composite molding process using the vacuum infusion method.

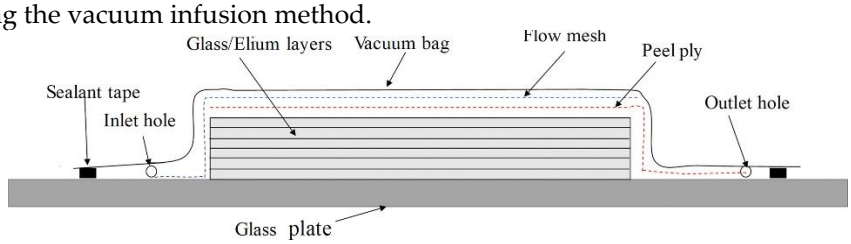

Figure 7. Vacuum infusion laminates steps [32].

In the vacuum infusion process, the fiber and flow media are placed on top of the mold and then closed using a vacuum bag film, then the air in the mold and composite is expelled into the atmosphere with the help of a vacuum compressor. This process will produce a composite that has a high matrix to reinforcement ratio, uniform mechanical properties, fewer voids, and uniform matrix thickness.

Below are the steps for the specimen manufacturing process:

1. Molding surface is cleaned from dirt and dust.
2. Carbon fiber layer is cut according to the width and the number of specimens.
3. Matrix preparation: Epoxy and hardener with a ratio of 1:1 is mixed in one container until homogeneous.
4. Preparation of molding process:
    a. Mirror glaze is applied in 3 layers on the surface of the mold evenly using a clean cloth.
    b. Carbon fiber is arranged in layers on top of the molding surface.
    c. Peel ply and flow media are cut to the size of carbon fiber
    d. Peel ply is lied just above the carbon fiber layer, then flow media is lied above two of them.
    e. Spiral hose is cut to arrange around the fiber pile, peel ply, flow media and connected by T-connector.
    f. Bagging film is holed to for T-connectors and spiral hoses access.
    g. All components are wrapped using bagging films. The specimen should be perfectly wrapped since bagging films act as a separating layer between the environment and the molding area where vacuum condition exists during the vacuum infusion process. Sealant tape is used to close any existing gap through the bagging films.
5. Preparation for vacuum infusion process: the T-connector that acts as outlet is connected to the resin reservoir tank using a tube, while the other T-connector that acts as inlet is connected to the matrix container. Another tube also connects the resin reservoir tank to the vacuum compressor.
6. Vacuum infusion process
    a. As vacuum compressor is turned on, the matrix will gradually move from the container to the molding space.
    b. When molding process has completed, vacuum compressor is turned off.
    c. The specimen will be left for drying process which lasts for 24 hours. After that, it can be taken off from the peel ply, flow media, and bagging films.
7. Specimen is cut according to each test standard using a water jet cutter. After the cutting, according to ASTM D638 procedure, the specimens were dried at room temperature at 23°C for 40 hours and 50% humidity.

Preprints (www.preprints.org) | NOT PEER-REVIEWED | Posted: 29 March 2022 doi:10.20944/preprints202203.0382.v1

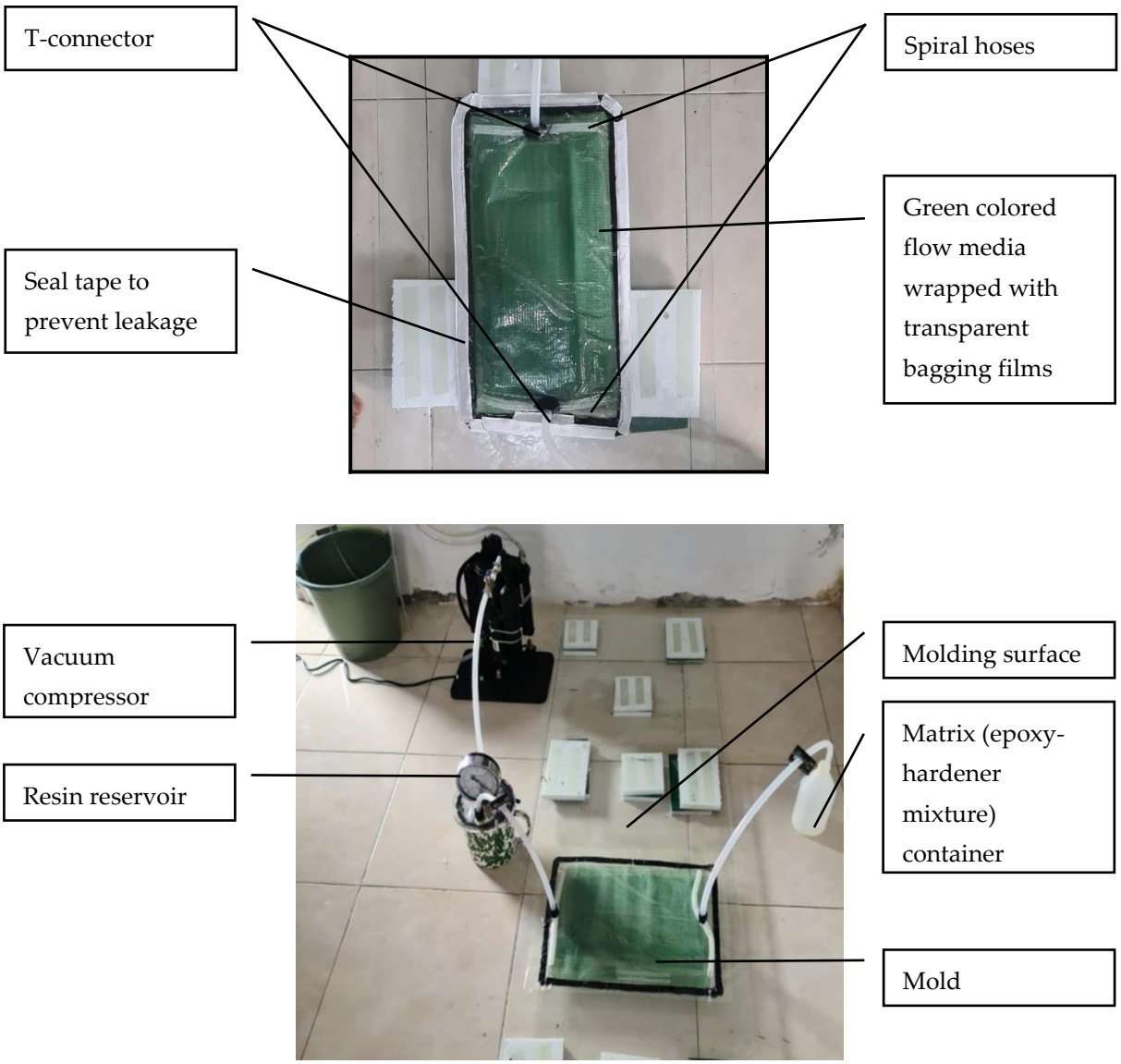

Figure 8. Vacuum infusion molding layout.

Figure 9. Vacuum infusion layout.

The specimens for each testing that have been manufactured is then divided into two categories: wet and dry specimens. Prior to mechanical testing, the wet specimen will go through a water absorption test. Specimens were immersed in 250 ml of water for 48 hours and dimensions and weight were measured every 6 hours. This test aims to determine the absorption of the material by knowing the size and weight change of the specimen after the immersion.

Preprints (www.preprints.org) | NOT PEER-REVIEWED | Posted: 29 March 2022 doi:10.20944/preprints202203.0382.v1

3. Results and Discussions

3.1. Water Absorption

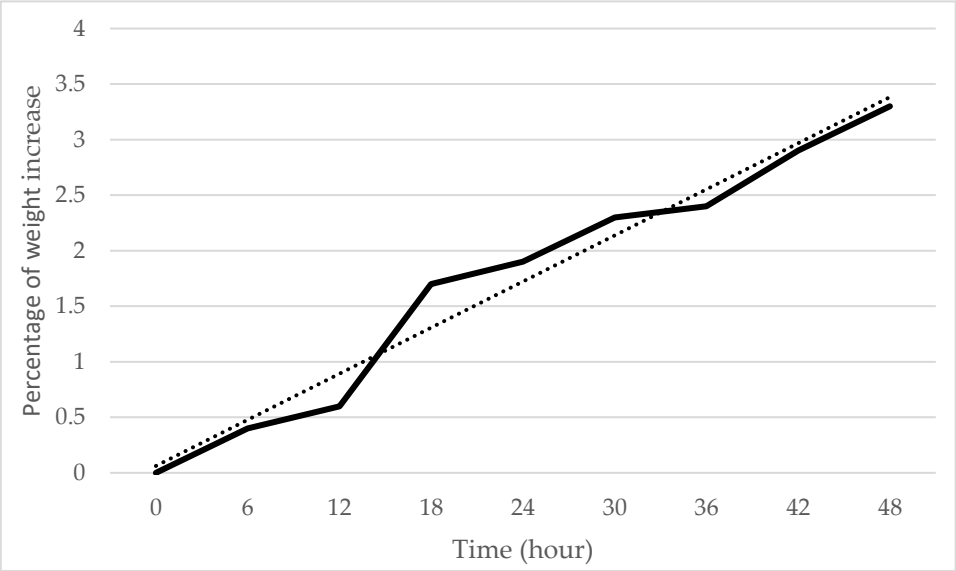

Figure 10. Specimen weight change over 48 hours of immersion.

Carbon fiber composite material has a water absorption capacity as shown in the graph. The specimens were immersed in fresh water for 48 hours and the weight was measured every 6 hours. Changes in weight that occur in each specimen tend to increase. In the first 6 hours the weight gain was 0.4%, the next 6 hours it was up 0.2%, and after that there was no significant increase in weight.

3.2. Tensile Analysis

3.2.1. Tensile Strength

Tensile testing was carried out to determine the maximum tensile strength of each specimen. The lowest tensile strength is observed to be 11.031 kN at the wet A' specimen.

Basah A'	Test date	Area mm²	Yield point kN	Max. Load kN	Break kN
		39.605	5.634	11.031	8.825

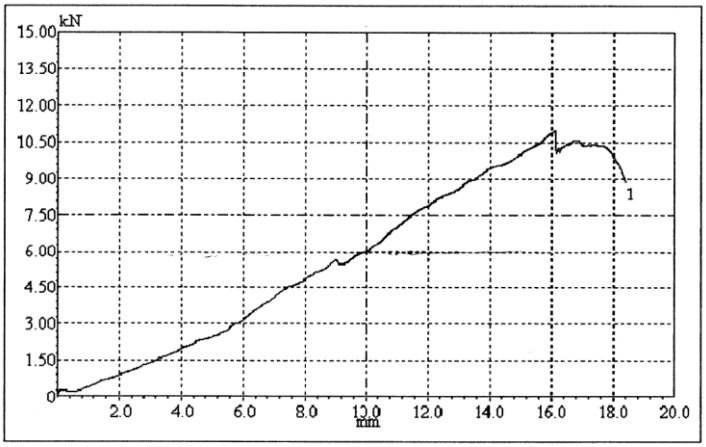

Figure 11. Tensile strength graph at wet A' specimen.

Preprints (www.preprints.org) | NOT PEER-REVIEWED | Posted: 29 March 2022 doi:10.20944/preprints202203.0382.v1

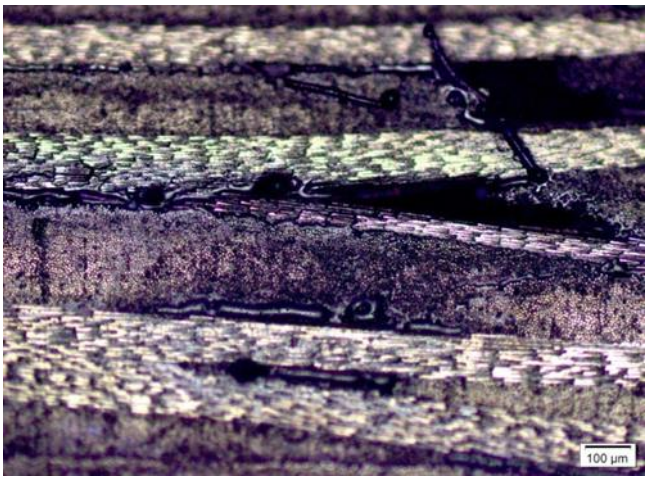

Figure 12. Microscopic structure of wet A' specimen.

Basah C'	Test date	Area mm²	Yield point kN	Max. Load kN	Break kN
		40.070	12.157	12.158	9.726

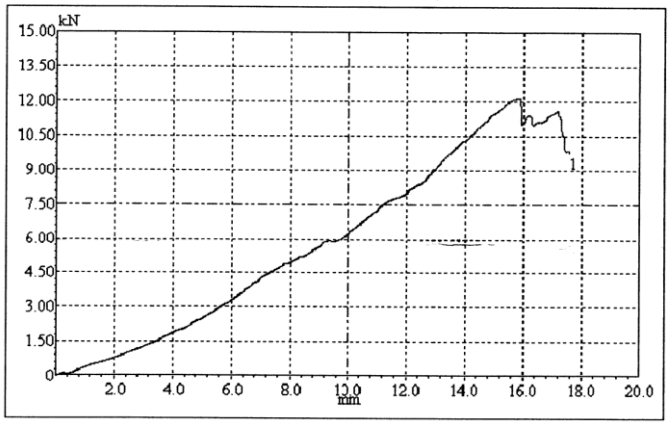

Figure 13. Tensile strength graph at wet C' specimen.

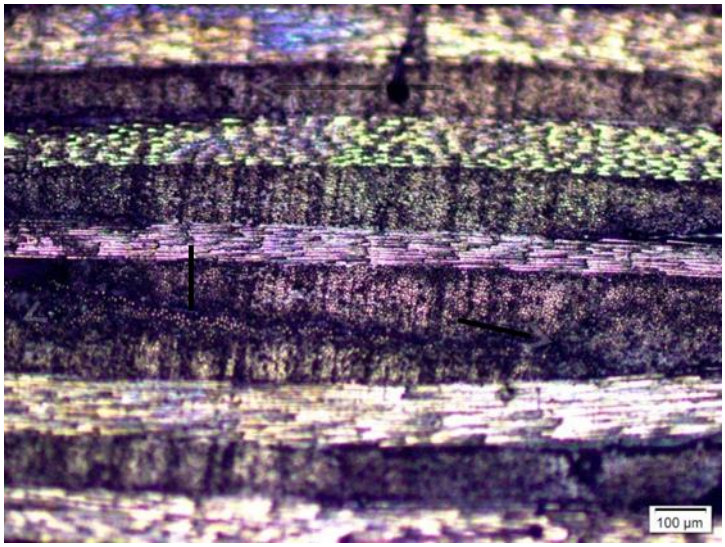

Figure 14. Microscopic structure of wet C' specimen.

Preprints (www.preprints.org) | NOT PEER-REVIEWED | Posted: 29 March 2022 doi:10.20944/preprints202203.0382.v1

As seen from Figure 12 of A' specimen, there are quite a lot of voids or contaminants compared to Figure 14 of C' specimen. These contaminants can affect the mechanical properties of the specimen. This statement is in line with Mallick's (2007) statement which says that the presence of voids in the composite can significantly reduce tensile, compressive, and flexural forces.

The table below is the complete data of all maximum tensile strengths observed at each specimen.

Table 6. Tensile strength of the specimens.

Dry Specimen			Wet Specimen		
No	Specimen	Tensile Strength	No	Specimen	Tensile Strength
1	A	12.126 kN	1	A'	11.031 kN
2	B	11.170 kN	2	B'	11.469 kN
3	C	11.838 kN	3	C'	12.158 kN
Average		11.711 kN	Average		11.552 kN

Table 6 shows that the average maximum tensile strength between types of specimens which has the highest value is the dry specimens. However, the value of the difference in the maximum tensile strength of the average type of specimen is really close to one another. The average tensile strength of the dry specimens compared to the wet specimens is only 1.38% higher. The average value of the maximum tensile strength of the wet specimen is lower because there is conditioning on the specimen before the tensile test is carried out, namely immersion in water. This is in line with the findings of Sadiwijantara (2019) which stated that the duration of immersion had a negative effect towards the composite tensile strength.

3.2.2. Tensile Stress

Table 7. Tensile stress of the specimens.

Dry Specimen			Wet Specimen		
No	Specimen	Tensile stress	No	Specimen	Tensile stress
1	A	301.140 MPa	1	A'	278.525 MPa
2	B	282.499 MPa	2	B'	275.690 MPa
3	C	300.038 MPa	3	C'	303.419 MPa
Average		294.559 MPa	Average		285.878 MPa

The highest tensile stress was found with a value of 303.419 MPa, and the lowest tensile stress was found at a value of 275.690 MPa. The highest average tensile stress value was found in the dry specimen with a value of 294.559 MPa, while the average value of the tensile stress in the wet specimen was 285.878 MPa.

3.2.3. Tensile Strain

The length increase data on the graph obtained from the tensile test cannot be used because of the lack of relevance of the data. Then a re-measurement of the specimens that have been tested using a vernier calliper with an accuracy of 0.01 mm was carried out, so that the length increase data was obtained as shown in table 8 below.

Preprints (www.preprints.org) | NOT PEER-REVIEWED | Posted: 29 March 2022 doi:10.20944/preprints202203.0382.v1

Table 8. Tensile strain of the specimens.

Dry Specimen			Wet Specimen		
No	Specimen	ΔL	No	Specimen	ΔL
1	A	0.14 mm	1	A'	0.15 mm
2	B	0.04 mm	2	B'	0.45 mm
3	C	0.16 mm	3	C'	0.08 mm

The results of the data obtained are useful for finding strain data that occurs in each specimen. With initial length of the specimen at 183 mm, it was found that the wet B' specimen has the highest tensile strain value at 0.00246 mm/mm while the lowest tensile strain value was 0.00022 mm/mm in dry B specimen.

3.2.4. Modulus of Elasticity

Table 9. Modulus of elasticity of the specimens.

Dry Specimen			Wet Specimen		
No	Specimen	Elasticity modulus	No	Specimen	Elasticity modulus
1	A	39.4×10^4 MPa	1	A'	34.0×10^4 MPa
2	B	129.2×10^4 MPa	2	B'	11.2×10^4 MPa
3	C	34.3×10^4 MPa	3	C'	69.4×10^4 MPa
Average		67.6×10^4 MPa	Average		38.2×10^4 MPa

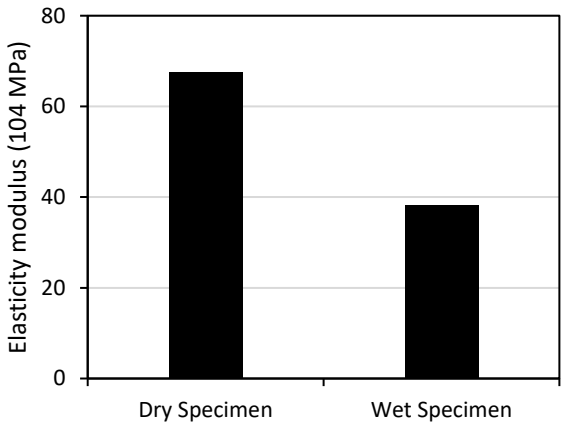

Figure 15. Average modulus of elasticity of both dry and wet specimens.

3.2.5. Fracture Characteristics

Microscopic photograph of the fracture of the dry specimen can be seen in Figure 16 below.

Preprints (www.preprints.org) | NOT PEER-REVIEWED | Posted: 29 March 2022 doi:10.20944/preprints202203.0382.v1

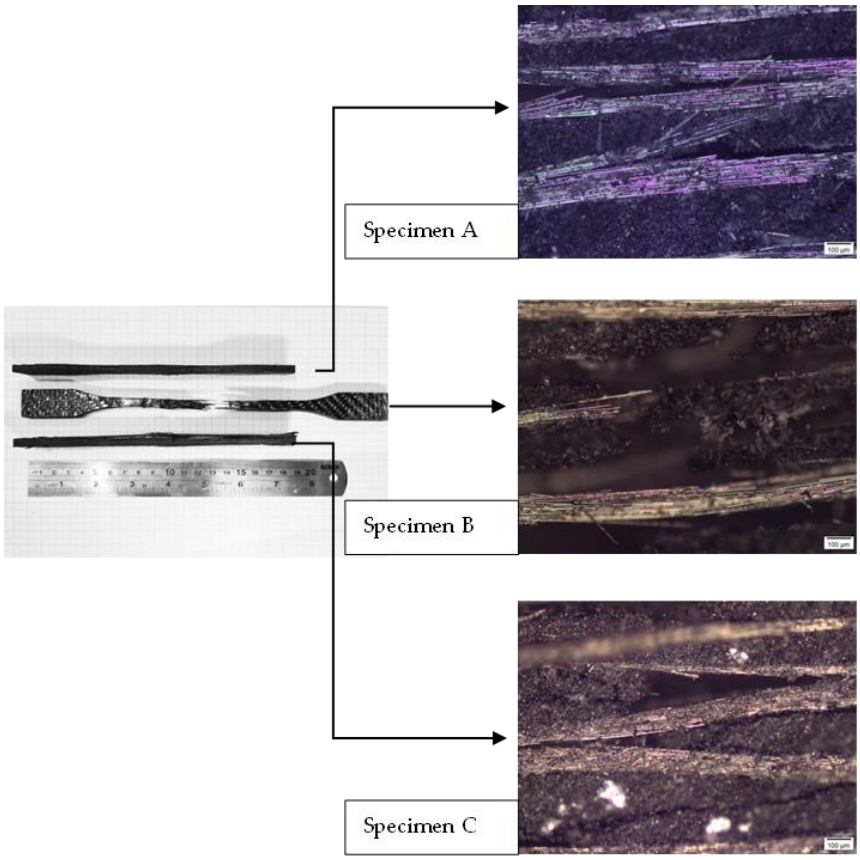

Figure 16. Microscopic photograph of each dry specimen.

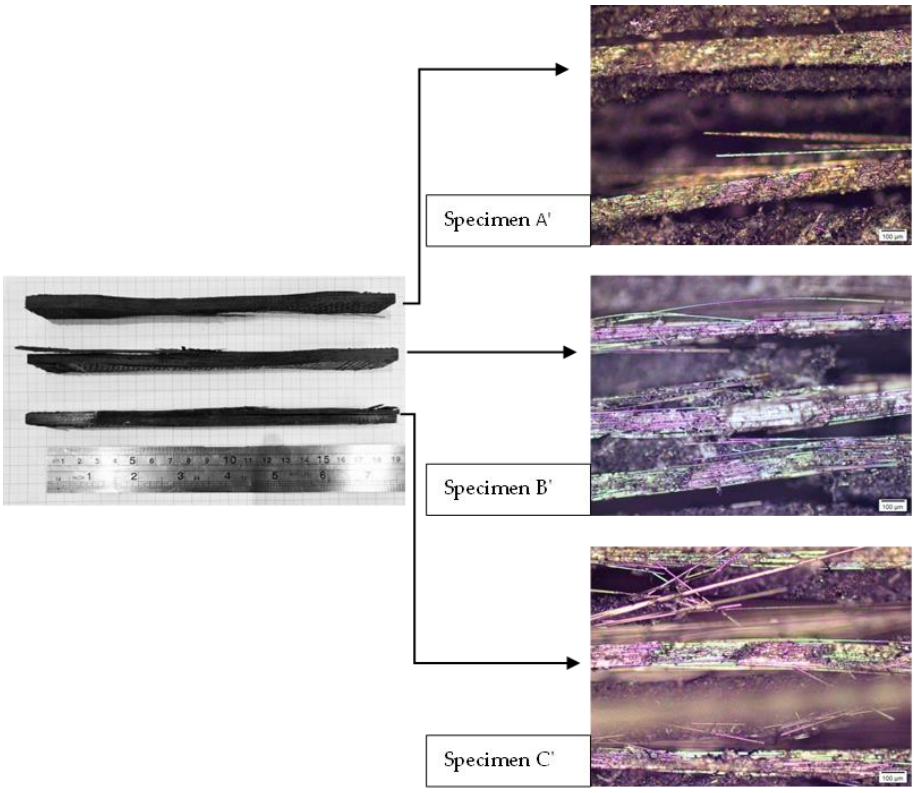

Figure 17. Microscopic photograph of each wet specimen.

Microscopic photograph is taken on the fracture area of the specimens to examine what happened when on the composite after the tensile test. It was found that many

Preprints (www.preprints.org) | NOT PEER-REVIEWED | Posted: 29 March 2022 doi:10.20944/preprints202203.0382.v1

specimens do not break when they reach maximum load, only part of the matrix is separated from the fiber bonds.

Based on the results of the physical analysis of the tensile test specimen, it can be concluded that the type of fracture that occurred in the specimen was classified according to the ASTM D3039 fracture character. Based on the table provided by ASTM D3039 to determine the fracture character, the type of fault in this study is XGM type, meaning that the specimen with XGM fault character has an X-explosive type of failure and a G-gage failure area (on the gage length section) and the fault location in the middle (M-middle) as can be seen in the figure below.

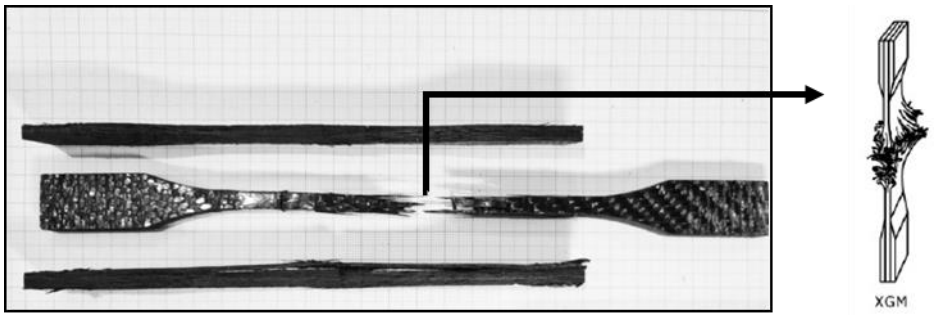

Figure 18. Fault characteristics of the specimen

The fault character can also be viewed from microscopic photographs to see the phenomena that occur in more detail in the fiber arrangement. The following image shows a microscopic photograph of the specimen.

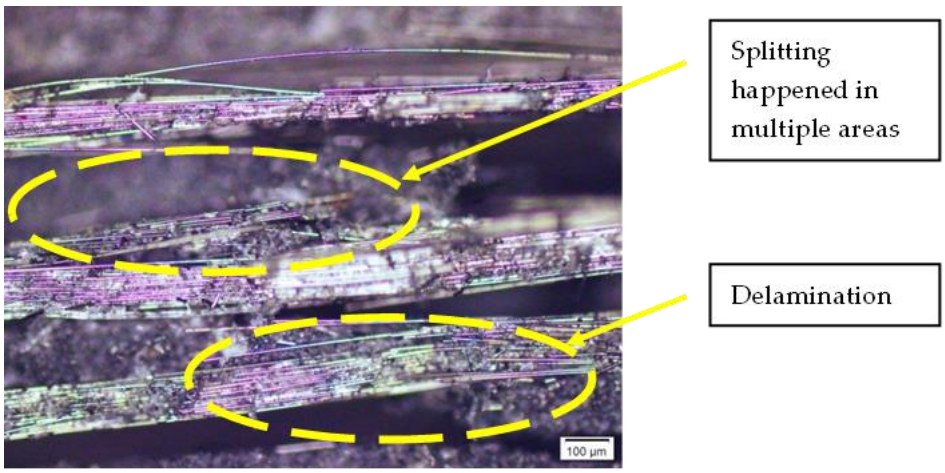

Figure 19. Microscopic photograph at the fracture location.

Figure 4.14 shows the fracture that occurs in the specimen. There are splitting faults in multiple areas where the fibers are separated from the webbing. There is also delamination between the fiber layers and the composite matrix where the fibers are split into small fragments and the layers between the fibers are separated (Raka and Mochamad 2018).

Preprints (www.preprints.org) | NOT PEER-REVIEWED | Posted: 29 March 2022 doi:10.20944/preprints202203.0382.v1

3.3. Bending Analysis

3.3.1. Bending Stress

The average value of the bending stress of the carbon fiber epoxy matrix composite material can be seen in table below.

Table 10. Bending stress of the specimens.

Dry Specimen			Wet Specimen		
No	Specimen	Bending Strength	No	Specimen	Bending Strength
1	A	213 MPa	1	A'	135 MPa
2	B	220 MPa	2	B'	141 MPa
3	C	188 MPa	3	C'	155 MPa
4	D	186 MPa	4	D'	151 MPa
5	E	167 MPa	5	E'	150 MPa
Average		195 MPa	Average		146 MPa

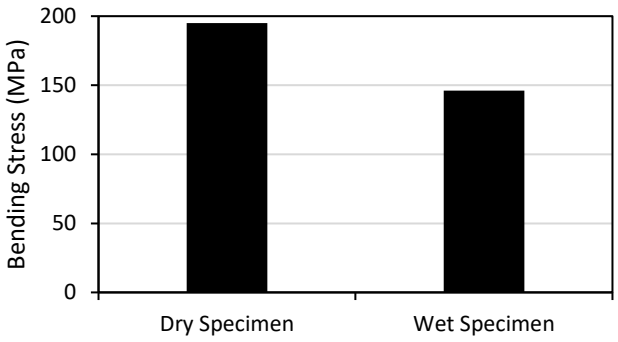

Figure 20. Average bending stress of both wet and dry specimens.

From the data above, it is known that the results of the bending test using the Zwick Roell machine, showed that the highest average stress value of 195 MPa was obtained from the dry specimen and the lowest average stress value was 146 MPa from the wet specimen. It was concluded that the immersion of the specimen did not significantly affect the ability of the specimen to withstand the applied stress but still tended to make the specimen weaker.

3.3.2. Bending Strain

The average value of the bending stress of the carbon fiber epoxy matrix composite material can be seen in the table below.

Table 11. Bending strain of the specimens.

Dry Specimen			Wet Specimen		
No	Specimen	Bending Strain	No	Specimen	Bending Strain
1	A	7.8	1	A'	8.2
2	B	7.2	2	B'	8.7
3	C	8.0	3	C'	8.6
4	D	8.1	4	D'	8.7
5	E	7.9	5	E'	8.7
Average		7.8	Average		8.6

Preprints (www.preprints.org) | NOT PEER-REVIEWED | Posted: 29 March 2022 doi:10.20944/preprints202203.0382.v1

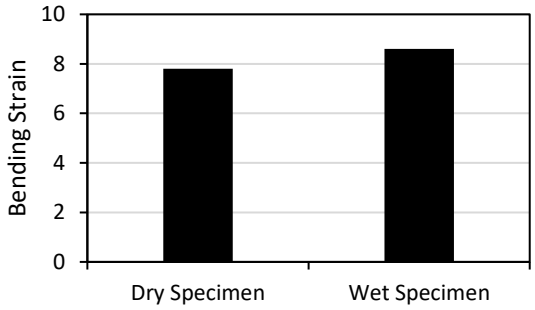

Figure 21. Bending strain of both wet and dry specimens.

It was found that the highest average strain was obtained from wet specimens of 8.6% and the lowest strain was 7.8%. From these data, it can be concluded that the immersion effect tends to affect the bending strain results, although the difference between the average values of the specimens is not significant.

3.3.3. Modulus of Elasticity

The average value of the bending modulus of elasticity of the carbon fiber epoxy matrix composite material can be seen in the table below.

Table 12. Modulus of elasticity of the specimens.

Dry Specimen			Wet Specimen		
No	Specimen	Elasticity Modulus	No	Specimen	Elasticity Modulus
1	A	8890 MPa	1	A'	5380 MPa
2	B	9680 MPa	2	B'	5480 MPa
3	C	7480 MPa	3	C'	6780 MPa
4	D	9860 MPa	4	D'	6190 MPa
5	E	8660 MPa	5	E'	6700 MPa
Average		8914 MPa	Average		6106 MPa

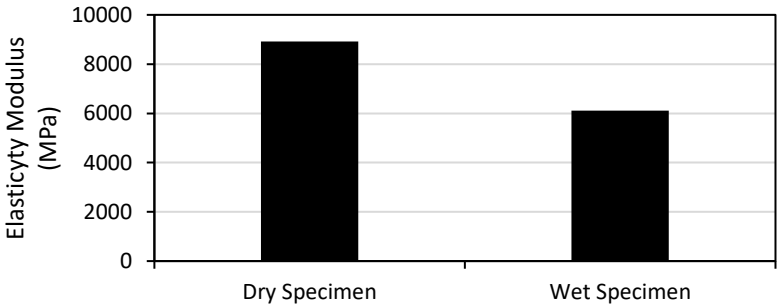

Figure 22. Average modulus of elasticity of both wet and dry specimens.

From the data obtained, the bending modulus of elasticity of these two specimens shows that the dry specimen has the largest modulus of elasticity with an average value of 8914 MPa and the smallest value of 6106 MPa in the wet specimen. It was concluded that the immersion effect had no effect on the modulus of elasticity of the specimen.

Based on the observation of the bending test data, it is known that the immersion effect of the composite has no effect on the bending stress and modulus of elasticity which results in a decrease in the stress and bending modulus of elasticity of the composite. Although there is a decrease in the bending stress and modulus of elasticity, the effect of immersion increases the average value of the strain on the wet specimen.

Preprints (www.preprints.org) | NOT PEER-REVIEWED | Posted: 29 March 2022 doi:10.20944/preprints202203.0382.v1

3.3.4. Fracture Characteristics

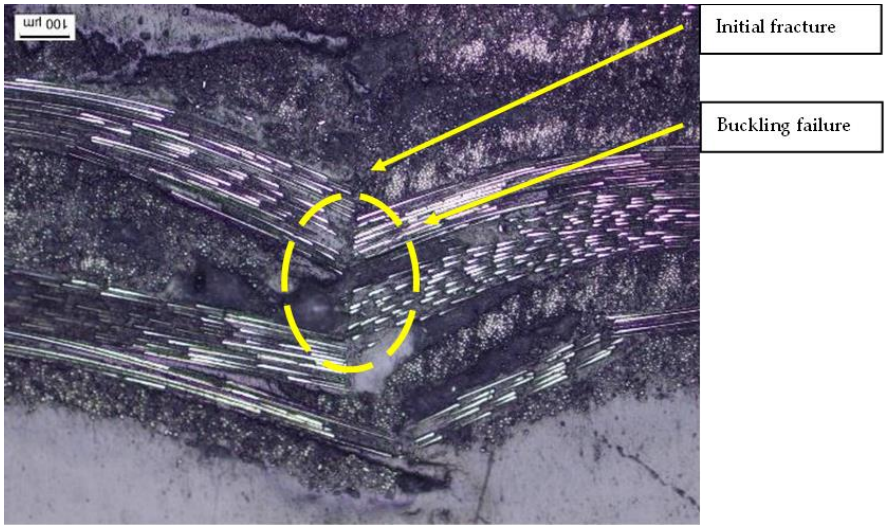

Figure 23. Fracture location at the dry specimen.

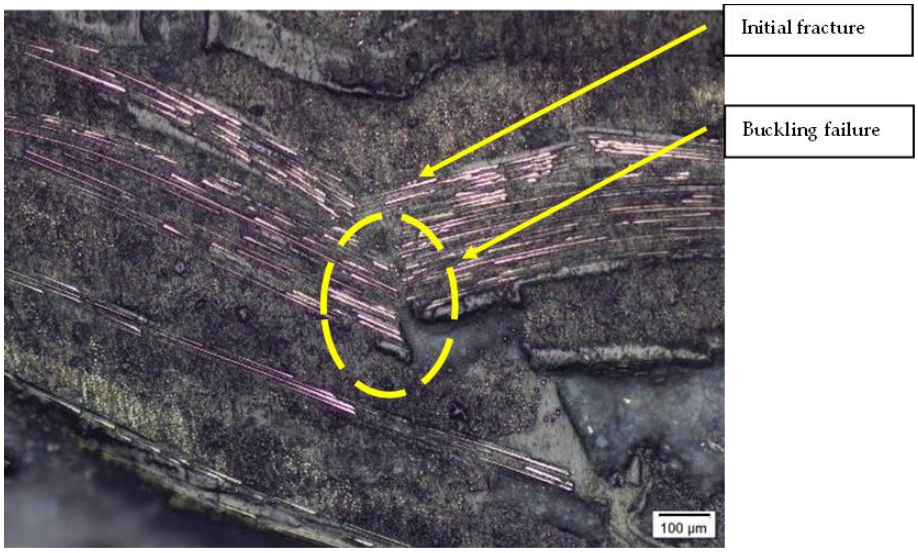

Figure 24. Fracture location at the wet specimen.

In wet specimens, the fracture experienced in the bending test specimen is in the center of the side surface. The predominant fault is the buckling fracture. This is because the fiber breaks due to tensile loads and the matrix is unable to accept the additional load.

3.4. Compression Analysis

In the compression test of carbon fiber composites, mechanical strengths such as composites are obtained such as compressive stress, compressive strain, and compressive elastic modulus. The test was carried out with a Zwick Roell test apparatus with a test speed of 1.3 mm/minute.

Preprints (www.preprints.org) | NOT PEER-REVIEWED | Posted: 29 March 2022 doi:10.20944/preprints202203.0382.v1

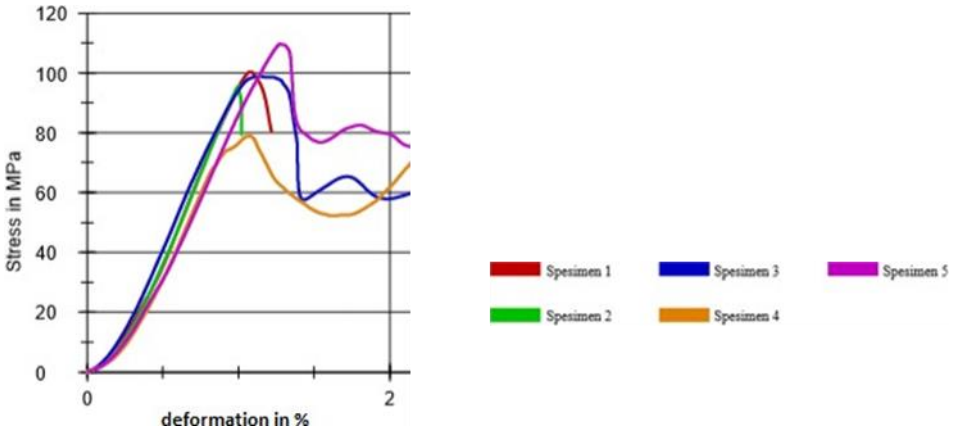

Figure 25. Compressive strength test result graph of the dry specimens.

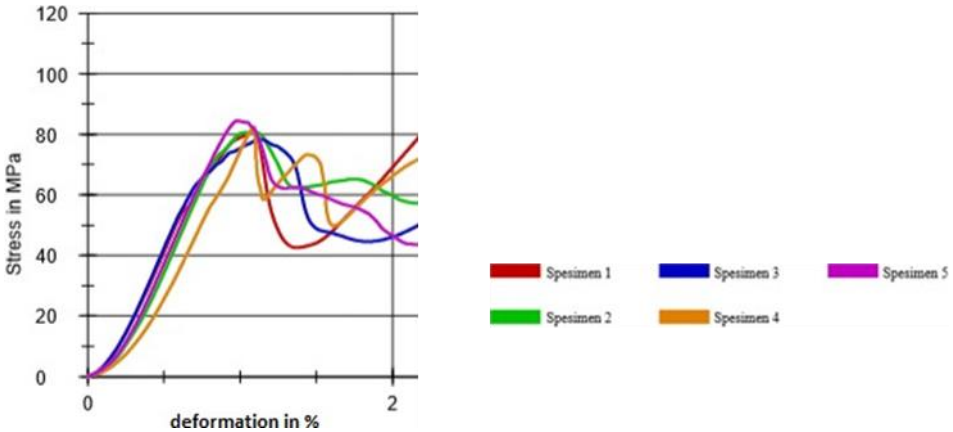

Figure 26. Compressive strength test result graph of the wet specimens.

3.4.1. Compressive Stress

Table 13. Compressive stress of the specimens.

Dry Specimen			Wet Specimen		
No	Specimen	Compressive Stress	No	Specimen	Compressive Stress
1	A	100.071 MPa	1	A'	80.080 MPa
2	B	95.045 MPa	2	B'	80.781 MPa
3	C	98.691 MPa	3	C'	78.178 MPa
4	D	77.960 MPa	4	D'	80.494 MPa
5	E	109.653 MPa	5	E'	84.419 MPa
Average		96.284 MPa	Average		80.790 MPa

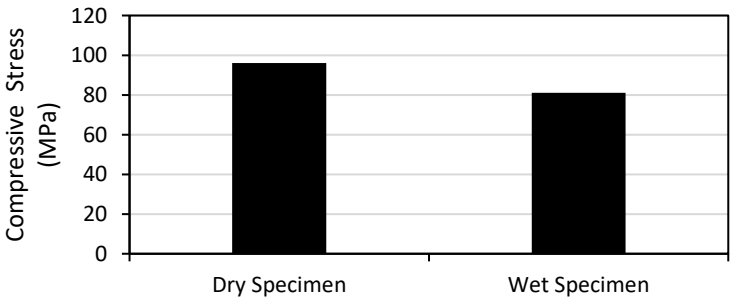

Figure 27. Average compressive stress of both wet and dry specimens.

Preprints (www.preprints.org) | NOT PEER-REVIEWED | Posted: 29 March 2022 doi:10.20944/preprints202203.0382.v1

Seen from the graph above, the average compressive stress on the wet and dry specimens shows the results where the dry specimen has a higher average stress value than the dry specimen. This shows that dry specimens are stronger in receiving loads than wet specimens. Wet specimens are weaker because the absorption that occurs causes water molecules to enter the cavities of the specimen, thus making the specimen weaker.

3.4.2. Compressive Strain

Table 14. Compressive strain of the specimens.

Dry Specimen			Wet Specimen		
No	Specimen	Compressive Strain	No	Specimen	Compressive Strain
1	A	0.00025	1	A'	0.00188
2	B	0.00038	2	B'	0.00175
3	C	0.00526	3	C'	0.00463
4	D	0.00376	4	D'	0.00388
5	E	0.00426	5	E'	0.00088
Average		0.00278	Average		0.00260

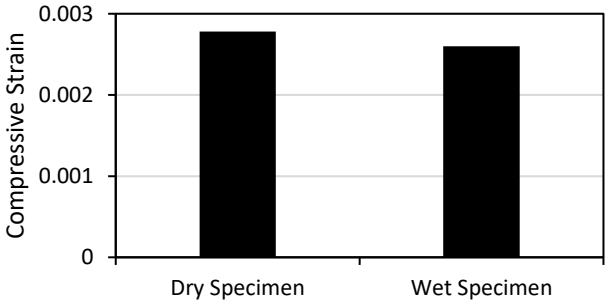

Figure 28. Average of compressive strain of both wet and dry specimens.

Seen from Figure 28, the average compressive strain on the wet and dry specimens shows the results where the dry specimen has a higher average stress value than the dry specimen. The ratio between the increase in length and the initial length was greater for dry specimens.

3.4.3. Modulus of Elasticity

Table 15. Modulus of elasticity of the specimens.

Dry Specimen			Wet Specimen		
No	Specimen	Elasticity Modulus	No	Specimen	Elasticity Modulus
1	A	40.0×10^4 MPa	1	A'	4.3×10^4 MPa
2	B	25.3×10^4 MPa	2	B'	4.6×10^4 MPa
3	C	18.8×10^4 MPa	3	C'	1.7×10^4 MPa
4	D	20.8×10^4 MPa	4	D'	2.1×10^4 MPa
5	E	25.7×10^4 MPa	5	E'	9.6×10^4 MPa
Average		14.3×10^4 MPa	Average		4.4×10^4 MPa

Preprints (www.preprints.org) | NOT PEER-REVIEWED | Posted: 29 March 2022 doi:10.20944/preprints202203.0382.v1

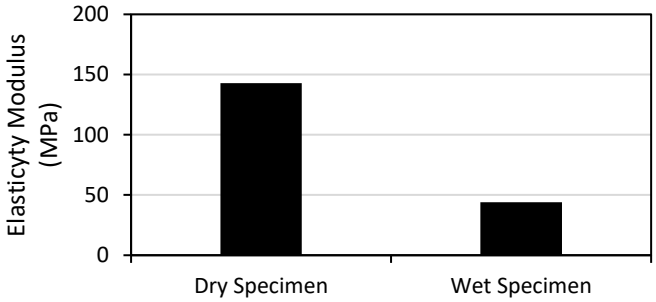

Figure 29. Average of elasticity modulus of both wet and dry specimens.

Seen from Graph 4.4, the average compressive strain on the wet and dry specimens shows the results where the dry specimen has a higher average stress value than the dry specimen. This shows that the ratio between compressive stress and compressive strain is higher for dry specimens than wet specimens.

3.4.4. Fracture Characteristics

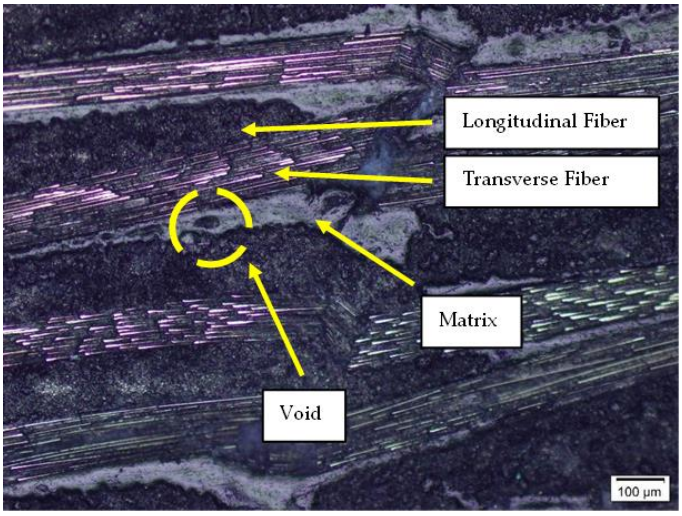

Figure 30. Microscopic photograph of dry B specimen.

The results of the micro-photos on the dry specimens occurred due to crack deflection caused by the position of the fibers on the inclined fault surface following the fault area, resulting in cracks following the inclined fiber position. Rich matrix is caused by the lack of fiber used and because the distribution of fibers in fiber printing is assembled separately, so that there is still a lot of free space without matrix and fiber bonds.

Preprints (www.preprints.org) | NOT PEER-REVIEWED | Posted: 29 March 2022 doi:10.20944/preprints202203.0382.v1

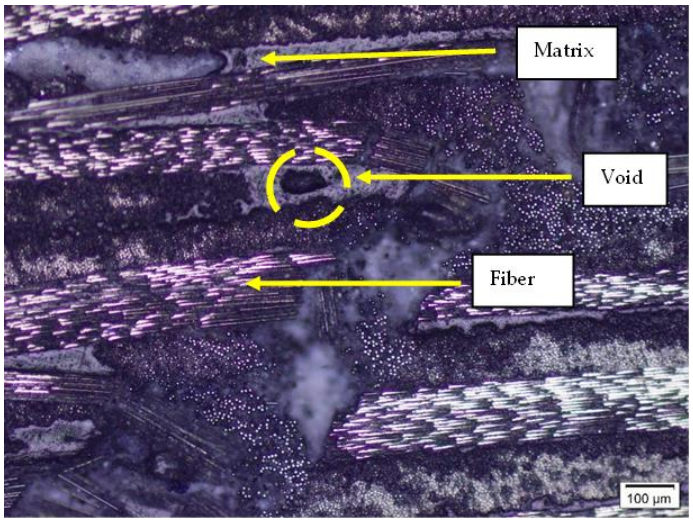

Figure 31. Microscopic photograph of wet D specimen.

The results of the micro-photo show that the fracture mode in the wet specimen is irregular. The rich matrix causes the fault. Rich matrix is caused by the lack of fiber used and because the distribution of fibers in fiber printing is assembled separately, so that there is still a lot of free space without matrix and fiber bonds. Faults in wet specimens are also affected because of the presence of voids which causes water to enter the voids so that the specimen will be more brittle, as can be seen in Figures 4.4 where there is more than one fracture point.

4. Conclusions

This study concluded that the immersion carried out on carbon/epoxy specimens for 48 hours showed an average percentage increase in final weight of 2.9%. This indicates that the immersion carried out did not significantly affect weight gain due to the material's solid structure, which resulted in low water absorption. From the tensile test, it can be concluded that the water absorption of the composite influences the tensile strength of the composite. The wet specimen has an average tensile stress of 285.878 MPa, lower than the dry specimen with an average tensile stress of 294.559 MPa. The results of micro-photo observations on the tensile test fracture show that there are delamination and splitting fractures in multiple areas. The fracture character that commonly occurs in all specimens is the XGM fracture character. The results of the bending test showed that the specimen that was not immersed was stronger, because the test results showed the highest stress value obtained was 220 MPa with an average of 195 MPa and the highest modulus of elasticity was 9860 MPa with an average of 8914 MPa in dry specimens, while the value of the test results the soaked specimen is smaller than the dry one. Immersion of the specimen for 48 hours influences the bending strain, this is obtained from the test results which show the highest value of 8.7% with an average of 8.6% from wet specimens, while dry specimens obtain a value of 8.1% with an average of 7.8%, although the strain value bending did not experience a significant increase due to the specimen immersion. The results of the observation of the micro test on the fracture part of the bending test specimen showed a buckling failure type of fault mode. This fault mode usually occurs because of the compressive load so that the fiber breaks and shifts. From the compression test, it was found that water absorption affects the compressive strength of the composite. Dry epoxy carbon fiber composites obtained an average stress result of 96.284 N/mm^2, with an average strain of 0.00278, and an average modulus of elasticity of 143471.76 MPa. While the carbon fiber composite epoxy matrix wet specimens obtained an average stress of 80.79 N/mm^2, with an average strain of 0.0026, and an average elastic modulus of 44508.703 MPa. It can be concluded that water absorption has a negative impact on the composite because wet specimens have lower compressive strength than dry specimens. The results of micro-photographs on the fractured part of the compression test specimen showed that

both specimens had a shear fracture characteristic. Dry specimens have more regular fracture results than wet specimens. The fracture modes observed in both specimens were matrix rich and crack debonding.

Author Contributions: Conceptualization, S and MAM; methodology, S, RAH, MAM; validation, S, MAM, and AH; formal analysis, S, AH, H, RAH, and MAM.; investigation, S, AH, H.; resources, S, H, and RAH; data curation, S, H, AH.; writing—original draft preparation, S, AH, and MAM.; writing—review and editing, S, AH, and MAM.; supervision, MAM.;. All authors have read and agreed to the published version of the manuscript."

Acknowledgments: The authros want to thank Mechanical and Industrial Engineering Department, Gadjah Mada University, and Mechanical Engineering Department, Universitas Muhammadiyah Yogyakarta for the collaboration research.

Conflicts of Interest: The authors declare no conflict of interest.

References

1. Khan, R. Fiber Bridging in Composite Laminates: A Literature Review. *Compos. Struct.* **2019**, *229*, doi:10.1016/j.compstruct.2019.111418.
2. Muflikhun, M.A.; Yokozeki, T. Steel Plate Cold Commercial - Carbon Fiber Reinforce Plastics Hybrid Laminates for Automotive Applications: Curing Perspective with Thermal Residual Effect. *J. Mater. Res. Technol.* **2021**, *14*, 2700–2714, doi:10.1016/j.jmrt.2021.07.152.
3. Muflikhun, M.A.; Yokozeki, T. Experimental and Numerical Analysis of CFRP-SPCC Hybrid Laminates for Automotive and Structural Applications with Cost Analysis Assessment. *Compos. Struct.* **2021**, *263*, 113707, doi:10.1016/j.compstruct.2021.113707.
4. Muflikhun, M.A.; Higuchi, R.; Yokozeki, T.; Aoki, T. The Evaluation of Failure Mode Behavior of CFRP/Adhesive/SPCC Hybrid Thin Laminates under Axial and Flexural Loading for Structural Applications. *Compos. Part B Eng.* **2020**, *185*, 107747, doi:10.1016/j.compositesb.2020.107747.
5. Rajak, D.K.; Wagh, P.H.; Linul, E. Manufacturing Technologies of Carbon/Glass Fiber-Reinforced Polymer Composites and Their Properties: A Review. *Polymers (Basel).* **2021**, *13*, doi:10.3390/polym13213721.
6. Muflikhun, M.A.; Higuchi, R.; Yokozeki, T.; Aoki, T. Delamination Behavior and Energy Release Rate Evaluation of CFRP/SPCC Hybrid Laminates under ENF Test: Corrected with Residual Thermal Stresses. *Compos. Struct.* **2020**, *236*, doi:10.1016/j.compstruct.2020.111890.
7. Muflikhun, M.A.; Higuchi, R.; Yokozeki, T.; Aoki, T. Failure Mode Analysis of CFRP-SPCC Hybrid Thin Laminates under Axial Loading for Structural Applications : Experimental Research on Strain Performance. *Compos. Part B Eng.* **2019**, *172*, 262–270, doi:10.1016/j.compositesb.2019.05.049.
8. Ganesarajan, D.; Simon, L.; Tamrakar, S.; Kiziltas, A.; Mielewski, D.; Behabtu, N.; Lenges, C. Hybrid Composites with Engineered Polysaccharides for Automotive Lightweight. *Compos. Part C Open Access* **2022**, *7*, 100222, doi:10.1016/j.jcomc.2021.100222.
9. Gibhardt, D.; Doblies, A.; Meyer, L.; Fiedler, B. Fatigue and Mechanical Properties of Glass Fibre Reinforced Epoxy. *Materials (Basel).* **2019**, *7*, 23.
10. Muflikhun, M.A. The Progressive Development Of Multifunctional Composite Materials In Different Applications. *Angkasa J. Ilm. Bid. Teknol.* **2020**, *12*, 9–18, doi:10.28989/angkasa.v12i2.673.
11. Muflikhun, M.A.; Yokozeki, T.; Aoki, T. The Strain Performance of Thin CFRP-SPCC Hybrid Laminates for Automobile Structures. *Compos. Struct.* **2019**, *220*, 11–18, doi:10.1016/j.compstruct.2019.03.094.
12. García-Moreno, I.; Caminero, M.Á.; Rodríguez, G.P.; López-Cela, J.J. Effect of Thermal Ageing on the Impact Damage Resistance and Tolerance of Carbon-Fibre-Reinforced Epoxy Laminates. *Polymers (Basel).* **2019**, *11*, 10–12, doi:10.3390/polym11010160.

13. Karger-Kocsis, J.; Mahmood, H.; Pegoretti, A. All-Carbon Multi-Scale and Hierarchical Fibers and Related Structural Composites: A Review. *Compos. Sci. Technol.* **2020**, *186*, doi:10.1016/j.compscitech.2019.107932.
14. Yang, S.; Cheng, Y.; Xiao, X.; Pang, H. Development and Application of Carbon Fiber in Batteries. *Chem. Eng. J.* **2020**, *384*, 123294, doi:10.1016/j.cej.2019.123294.
15. Reder, C.; Loidl, D.; Puchegger, S.; Gitschthaler, D.; Peterlik, H.; Kromp, K.; Khatibi, G.; Betzwar-Kotas, A.; Zimprich, P.; Weiss, B. Non-Contacting Strain Measurements of Ceramic and Carbon Single Fibres by Using the Laser-Speckle Method. *Compos. Part A Appl. Sci. Manuf.* **2003**, *34*, 1029–1033, doi:10.1016/S1359-835X(03)00240-9.
16. Ueda, M.; Tasaki, Y.; Kawamura, C.; Nishida, K.; Honda, M.; Hattori, K.; Miyanaga, T.; Sugiyama, T. Estimation of Axial Compressive Strength of Unidirectional Carbon Fiber Reinforced Plastic Considering Local Fiber Kinking. *Compos. Part C Open Access* **2021**, *6*, 100180, doi:10.1016/j.jcomc.2021.100180.
17. Hsissou, R.; Seghiri, R.; Benzekri, Z.; Hilali, M.; Rafik, M.; Elharfi, A. Polymer Composite Materials: A Comprehensive Review. *Compos. Struct.* **2021**, *262*, 0–3, doi:10.1016/j.compstruct.2021.113640.
18. Alhayek, A.; Syamsir, A.; Bakar, A.; Supian, M.; Usman, F.; Rizal, M.; Asyraf, M.; Atiqah, M.A. Flexural Creep Behaviour of Pultruded GFRP Composites Cross-Arm : A Comparative Study on the Effects of Stacking Sequence. *Polymers (Basel).* **2022**, *14*, 1–15.
19. Tin, H.X.; Thuy, N.T.; Seo, S.Y. Structural Behavior of RC Column Confined by FRP Sheet under Uniaxial and Biaxial Load. *Polymers (Basel).* **2022**, *14*, doi:10.3390/polym14010075.
20. Vashchuk, A.; Kobzar, Y. Chemical Welding of Polymer Networks. *Mater. Today Chem.* **2022**, *24*, 100803, doi:10.1016/j.mtchem.2022.100803.
21. Li, Q.; Shen, H.X.; Liu, C.; Wang, C.F.; Zhu, L.; Chen, S. Advances in Frontal Polymerization Strategy: From Fundamentals to Applications. *Prog. Polym. Sci.* **2022**, *127*, 101514, doi:10.1016/j.progpolymsci.2022.101514.
22. Frigione, M.E.; Mascia, L.; Acierno, D. Oligomeric and Polymeric Modifiers for Toughening of Epoxy Resins. *Eur. Polym. J.* **1995**, *31*, 1021–1029, doi:10.1016/0014-3057(95)00091-7.
23. Dong, M.; Zhang, H.; Tzounis, L.; Santagiuliana, G.; Bilotti, E.; Papageorgiou, D.G. Multifunctional Epoxy Nanocomposites Reinforced by Two-Dimensional Materials: A Review. *Carbon N. Y.* **2021**, *185*, 57–81, doi:10.1016/j.carbon.2021.09.009.
24. Hsissou, R. Review on Epoxy Polymers and Its Composites as a Potential Anticorrosive Coatings for Carbon Steel in 3.5% NaCl Solution: Computational Approaches. *J. Mol. Liq.* **2021**, *336*, 116307, doi:10.1016/j.molliq.2021.116307.
25. Sunardi, S.; Fawaid, M.; Lusiani, R.; Cahyadi, C. Pengaruh Arah Serat Komposit Serat Daun Pandan Duri Dengan Matrik Polyester Terhadap Kekuatan Tarik Dan Kekuatan Impak Untuk Aplikasi Body Kendaraan Motor. *Tek. J. Sains dan Teknol.* **2014**, *10*, 151, doi:10.36055/tjst.v10i2.6675.
26. Kaddami, H.; Hafs, O.; Assimi, T.E.L.; Boulafrouh, L.; Ablouh, E.H.; Mansori, M.; Banouni, H.; Bouzit, S.; Erchiqui, F.; Benmoussa, K.; et al. Implementation and Characterization of a Laminate Hybrid Composite Based on Palm Tree and Glass Fibers. *Polymers (Basel).* **2021**, *13*, 1–17, doi:10.3390/polym13193444.
27. Vo, H.N.; Pucci, M.F.; Drapier, S.; Liotier, P.J. Capillary Pressure Contribution in Fabrics as a Function of Fibre Volume Fraction for Liquid Composite Moulding Processes. *Colloids Surfaces A Physicochem. Eng. Asp.* **2022**, *635*, doi:10.1016/j.colsurfa.2021.128120.
28. Pramono, G.E.; Sutisna, S.P. PERBANDINGAN KARAKTERISTIK SERAT KARBON ANTARA METODE MANUAL LAY-UP DAN VACUUM INFUSION DENGAN PENGGUNAAN FRAKSI BERAT SERAT 60%. *J. Ilm. Tek. Mesin* **2017**, *03*, 1–6.
29. Standard Test Method for Tensile Properties of Plastics, ASTM Standard D-638-08.
30. Standard Test Method for Tensile Properties of Polymer Matrix Composite Materials, ASTM D-3039.
31. Standard Test Method for Compressive Properties of Rigid Plastics, ASTM D695., doi:10.1520/D0695-15.2.
32. Han, N.; Baran, I.; Zanjani, J.S.M.; Yuksel, O.; An, L.L.; Akkerman, R. Experimental and Computational Analysis of the Polymerization Overheating in Thick Glass/Elium® Acrylic Thermoplastic Resin Composites. *Compos. Part B Eng.* **2020**, *202*, 108430, doi:10.1016/j.compositesb.2020.108430.

 doi:10.20944/preprints202203.0382.v1